HHS Public Access

Author manuscript

Eur J Neurosci. Author manuscript; available in PMC 2018 October 05.

Published in final edited form as:

Eur J Neurosci. 2017 October ; 46(8): 2416–2425. doi:10.1111/ejn.13707.

Altered Cav1.2 function in the Timothy Syndrome mouse model produces ascending serotonergic abnormalities

Daniel G. Ehlinger[1,2,*] and **Kathryn G. Commons**[1,2]

[1]Department of Anesthesiology, Perioperative and Pain Medicine, Boston Children's Hospital, 300 Longwood Ave, Boston, MA 02115, USA

[2]Department of Anesthesia, Harvard Medical School, 300 Longwood Ave, Boston, MA 02115, USA

Abstract

Polymorphism in the gene *CACNA1C*, encoding the pore-forming subunit of Cav1.2 L-type calcium channels, has one of the strongest genetic linkages to schizophrenia, bipolar disorder, and major depressive disorder: psychopathologies in which serotonin signaling has been implicated. Additionally, a gain-of-function mutation in *CACNA1C* is responsible for the neurodevelopmental disorder Timothy Syndrome that presents with prominent behavioral features on the autism spectrum. Given an emerging role for serotonin in the etiology of autism spectrum disorders, we investigate the relationship between Cav1.2 and the ascending serotonin system in the Timothy Syndrome type 2 (TS2-neo) mouse, which displays behavioral features consistent with the core triad of ASD. We find that TS2-neo mice exhibit enhanced serotonin tissue content and axon innervation of the dorsal striatum, as well as decreased serotonin turnover in the amygdala. These regionally specific alterations are accompanied by an enhanced active coping response during acute stress (forced-swim), serotonin neuron Fos-activity in the caudal dorsal raphe, and serotonin type 1A receptor dependent feedback-inhibition of the rostral DRN. Collectively, these results suggest that the global gain of function Cav1.2 mutation associated with Timothy Syndrome has pleotropic effects on the ascending serotonin system including neuroanatomical changes, regional differences in forebrain serotonin metabolism and feedback regulatory control mechanisms within the dorsal raphe. Altered activity of the ascending serotonin system continues to emerge as a common neural signature across several ASD mouse models, and the capacity for Cav1.2 L-type calcium channels to impact both serotonin structure and function has important implications for several neuropsychiatric conditions.

Graphical Abstract

[*]Correspondence to Dr. Daniel G. Ehlinger, daniel.ehlinger@childrens.harvard.edu, phone: 617-919-4271.
DR. DANIEL GAVIN EHLINGER (Orcid ID : 0000-0001-9116-3996)

Conflict of Interest Statement

KGC has received compensation from Zogenix, Inc. for professional services unrelated to the contents of the manuscript. DGE declares no potential conflicts of interest.

Author Contributions

DGE and KGC designed the experiments and analyzed the data. DGE collected the data and wrote the paper.

Data Accessibility Statement

On acceptance for publication all associated data will be deposited on the website figshare.com

The Timothy Syndrome mouse carries a mutation in *Cacna1c* that encodes Cav1.2 L-type calcium channels. We reveal enhanced serotonin axon innervation of the dorsal striatum, decreased turnover in the amygdala, and disrupted dorsal raphe serotonin neuron activity/feedback-inhibition in this model. This represents an important step in understanding serotonin dysfunction in autism, and the impact of Cav1.2 on the serotonin system has important implications for several neuropsychiatric conditions.

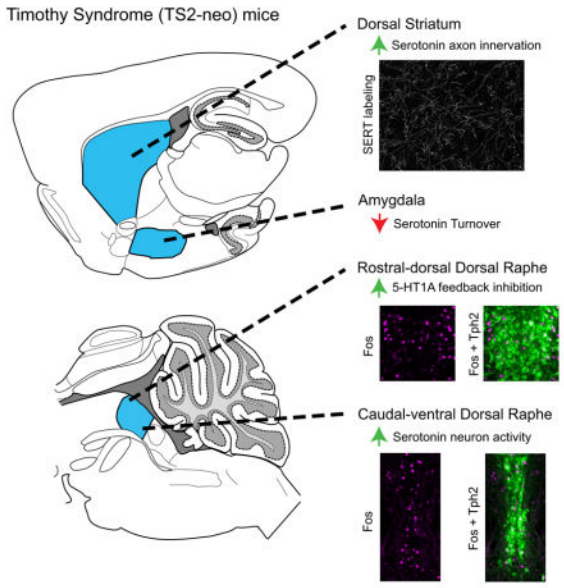

Keywords

Serotonin; Autism; Neurodevelopment; 5-HT1A; dorsal raphe nucleus

Introduction

Autism spectrum disorders (ASD) are a heterogeneous group of neurodevelopmental disorders characterized by abnormal social behavior, communication deficits, and restricted interests/repetitive behavior (stereotypy) (Levy *et al.*, 2009). While the precise causes of ASD are unknown in the majority of clinical cases, an extremely wide range of genetic and environmental factors has been shown to influence both the development and expression of ASD, and numerous cases of monogenic disorders have been revealed that present with autism-like behavior. A common neural circuit that is disrupted across ASD has yet to be identified, and its identification would support the development of targeted treatments to alleviate behavioral impairments that are characteristic of the disorder.

Interest in serotonin (5-hydroxytryptamine; 5-HT) system involvement in ASD originated with the discovery of elevated blood serum 5-HT levels in a high percentage of ASD patients (Schain & Freedman, 1961; Muller *et al.*, 2016). More recently, several mouse models with genetic mutations that directly influence neural serotonergic transmission display behavioral impairments that are reminiscent of human ASD behaviors, including mice with the human

Ala56 SLC6A4 allele (altering 5-HT transporter function) (Kerr *et al.*, 2013; Veenstra-VanderWeele *et al.*, 2012) and tryptophan hydroxylase 2 (Tph2) knockout mice (disrupted 5-HT production) (Kane *et al.*, 2012; Mosienko *et al.*, 2015). Additionally, the inbred BTBR mouse strain, commonly used as a model of idiopathic ASD due to its unique behavioral profile of reduced social interaction and increased repetitive behaviors, displays altered 5-HT forebrain tissue content, 5-HT axon density, 5-HT type 1A receptor (5-HT1A) function, and increased dorsal raphe 5-HT neuron activity (Gould *et al.*, 2011; Guo & Commons, 2016). These results suggest that 5-HT system abnormalities may be highly prevalent in mouse models of ASD and could represent a commonly disrupted neural circuit across the disorder.

Human polymorphism in noncoding regions of *CACNA1C*, which codes for the alpha-1 pore-forming subunit of the CaV1.2 L-type calcium channel, have been strongly associated with an increased risk to develop a broad range of neuropsychiatric disorders with potential 5-HT system involvement, including depression, schizophrenia, and bipolar disorder (Green *et al.*, 2010; Cross-Disorder Group of the Psychiatric Genomics Consortium, 2013). This gene is also implicated in the severe neurodevelopmental disorder Timothy Syndrome, in which a gain of function single nucleotide polymorphism (G406R) in exon 8/8A of *CACNA1C* results in a functional channel with disrupted inactivation and an extremely high penetrance of ASD (Splawski *et al.*, 2004; Splawski *et al.*, 2005). Importantly, L-type calcium channels are known to directly regulate local dendritic 5-HT release within the dorsal raphe nuclei (DRN), the major source of forebrain 5-HT, that typically provides feedback-inhibitory control over 5-HT neuron activity through 5-HT type 1A receptors (5-HT1A) (Colgan *et al.*, 2012). Therefore, both differential expression and dysfunction of *CACNA1C*/Cav1.2 L-type calcium channels could potentially influence the etiology of a broad range of neuropsychiatric and neurodevelopmental disorders through its actions on the ascending 5-HT system.

In light of this, the recently developed Timothy Syndrome Type 2 mouse model of ASD (TS2-neo) emerges as a particularly interesting genetic mouse model through which to explore alterations in 5-HT system structure and function that may occur downstream of *CACNA1C* disruption. Heterozygous TS2-neo mice contain the gain of function allele accompanied by an un-excised neomycin-resistance cassette that suppresses mutant channel expression, resulting in normal survival of mice. TS2-neo mice display behavioral abnormalities that are reminiscent of the core triad of human ASD symptomology: repetitive behavior, communication deficits, and impaired social interaction (Bader *et al.*, 2011). In the present study we assess 5-HT system structure and function in the TS2-neo mouse, including forebrain monoamine/metabolite tissue content and 5-HT axon density within forebrain regions implicated in the etiology of ASD, behavioral response to an acute forced swim stress that potently activates the DRN ascending 5-HT system, and the pattern of DRN 5-HT neural Fos activity and 5-HT1A dependent feedback inhibition.

Materials and Methods

Mice

All procedures were approved by the Boston Children's Hospital Institutional Animal Care and Use Committee. Heterozygous B6.Cg-Cacna1ctm2Itl/J (G406R/TS2-neo; stock #019547) and c57BL/6J (Wild-type/WT; stock #000664) breeding pairs were purchased from the Jackson Laboratory (Bar Harbor, ME). First generation progeny from male TS2-neo and female WT mice were born at Boston Children's Hospital. Only male TS2-neo mice were used for breeding as to avoid potential disruptions in maternal behavior in TS2-neo females that would confound subsequent experimental results. Progeny were used as subjects at postnatal day (P) 28 ± 1, representing a periadolescent time-period (Laviola *et al.*, 2003) that is more relevant to the corresponding human condition that manifests in childhood. Postnatal 5-HT system development has largely completed by this age (Lidov & Molliver, 1982; Liu & Wong-Riley, 2010), although additional refinements may occur with aging over the lifespan. Euthanasia of subjects used for neurochemical analyses are described in subsequent sections. Additional subjects not used for neurochemical analyses were euthanized via CO_2 exposure.

Forced swim test

A forced swim test (FST) was used to assess stress coping behavior, which is disrupted across several mouse models of ASD and impacts ascending 5-HT neuron functional activity and 5-HT1A dependent feedback-inhibition. TS2-neo and WT mice were randomly assigned to treatment groups, weighed, and injected subcutaneously with either saline (0.9% NaCl) or WAY-100635 (WAY) (Sigma-Aldrich #W108) at 0.4 mg/kg (Fletcher *et al.*, 1996). Mice were returned to their home cage for ten minutes before placement into a cylindrical glass tank (46cm high × 20cm diameter) filled 20cm deep with water (25 ± 1° C) for 15 minutes and videotaped for subsequent behavioral analysis. No overall differences in weight were observed between TS2-neo and WT mice (male or female). Swimming (active coping; horizontal movement through tank with both hindpaws moving in synchrony) and immobility (passive coping; minimal horizontal movement and minimal hindpaw movements required to keep the head above the water) behaviors were scored using a 5-second time interval sampling method (Cryan *et al.*, 2005). Immediately after the swim, mice were removed from the tank, quickly towel dried, and returned to their home cage. To initially assess genotype and sex differences in swim behavior, N = 40 saline injected WT (male, n = 9; female, n = 9) and TS2-neo (male, n = 11; female, n = 11) mice were used. Data was analyzed by mixed ANOVA with genotype and sex and between-subjects factors and 5-minute time bin as a within subject factor. Post-hoc bonferonni corrected t-tests were assessed on each individual 5-minute time bin. This analysis revealed no main effects of sex or interactions between sex and genotype on swim behavior, therefore subsequent analysis was sex balanced but underpowered to assess sex differences. For WAY treatment in the FST, N = 20 (TS2-neo, n = 11; WT, n = 9) mice were used and compared to saline treated mice by mixed-ANOVA (between-groups factors of genotype and drug; within-subjects factor of 5-minute time bin) with post-hoc bonferonni corrected t-tests on each individual 5-minute time bin.

Locomotor activity

Locomotor activity was assessed in a separate set of TS2-neo (n =7) and WT (n=6) mice in an open-field apparatus (Photobeam Activity System, San Diego Instruments, San Diego, CA). Within clear plexiglass cages (25 cm width × 48 cm length ×20 cm height), accumulated beam breaks were automatically counted, and included ambulatory, fine and rearing movements over three time bins of 5 minutes for a total of 15 minutes. Movement measures were totaled within each time bin to acquire a total locomotor activity score. Additionally, total movement within the center rectangle (13 cm width × 24 cm length) of the open-field was calculated separately. Locomotor activity data was analyzed using mixed-ANOVA with time as a repeated measure and genotype as a between subjects factor. Accumulated beam breaks were automatically counted, and included ambulatory, fine and rearing movements over three time bins of 5 minutes for a total of 15 minutes, and analyzed via mixed-ANOVA.

HPLC analysis

Forebrain tissue content of monoamines and their metabolites, including serotonin (5-HT), the 5-HT metabolite 5-Hydroxyindoleacetic acid (5-HIAA), norepinephrine, dopamine, and the dopamine metabolites DOPAC and HVA, were measured from a final set of N = 19 mice (TS2-neo, n = 9; WT, n = 10) that had not been previously exposed to the FST. Animals were anesthetized with isofluorane and quickly decapitated for brain extraction. Whole brains were snap-frozen in isopentane cooled with dry ice. Serial 300μm sections were cut on a cryostat, and 2 mm diameter tissue punches were taken from forebrain regions with known involvement in ASD (Bachevalier & Loveland, 2006; Fuccillio, 2016) and that have 5-HT axon termination fields with distinct areas of origin within the raphe nuclei (Commons, 2016): the orbitofrontal cortex, dorsal striatum, dorsal hippocampus, and amygdala. Following tissue collection, samples were analyzed by the Neurochemistry Core Facility at Vanderbilt University. Briefly, frozen brain tissue samples were homogenized by using a tissue dismembrator (Misonix XL-2000; Qsonica) in a solution containing 100 mM TCA, 10 mM NaC2H3O2, 100 μM EDTA, 5 ng/mL isoproterenol (an internal standard), and 7.5% (vol/vol) methanol (pH 3.8). Using a Waters 2707 autosampler, 10 μL of supernatant from each sample was injected onto a Phenomenex Kintex (2.6 μm, 100 A) C18 HPLC column (100 mm × 4.6 mm). Biogenic amines were eluted with a mobile phase [100 mM TCA, 10 mM NaC2H3O2, 100 μM EDTA, and 7.5% methanol (pH 3.8)] delivered at 0.6 mL/min by using a Waters 515 HPLC pump. Analytes were detected by using an Antec Decade II (oxidation: 0.4) electrochemical detector operated at 33 °C. Empower software was used to manage HPLC instrument control and data acquisition. Data were analyzed by Mixed-ANOVA (genotype × region) and post-hoc independent samples t-tests controlling for error inflation using a false discovery rate (FDR) (Benjamani & Hochberg, 1995) of 5%, based on the six monoamines/metabolites compared within each brain regions. FDR-adjusted p-values (q) are reported alongside raw p-values.

Immunofluorescence

Saline and WAY-100635 (WAY) treated mice used in the FST were used for subsequent immunofluorescence experiments. For serotonin transporter (SERT) axon density

experiments, saline-treated TS2-neo (n = 6) and WT (n = 6) were anesthetized with an overdose of sodium pentobarbital and perfused intracardially with approximately 5 ml 0.9% saline followed by approximately 50 ml of 4.0% paraformaldehyde in 0.1 M phosphate buffer immediately following the FST. For Fos/Tph2 colabeling experiments, saline treated (TS2-neo, n = 14; WT, n = 12) and WAY treated mice (TS2-neo, n = 9; WT, n = 9) were perfused precisely 120 minutes after the FST to allow for the expression and accumulation of Fos protein. Brains were removed and stored in the same 4.0% PFA solution overnight and then equilibrated in a solution of 30% sucrose in 0.1 M phosphate buffer (4° C), then frozen and sectioned 40 μm thick. Immunofluorescence processing was performed on floating sections. SERT was detected by incubating sections in primary antisera raised in rabbit (SERT, Calbiochem, catalog PC177L) diluted 1:1000 in 0.1 M phosphate buffered saline (PBS) with 0.3% Triton X-100, 0.1% bovine serum albumin and 0.01% sodium azide (PBS-BSA-TA) at 4° C for 72 hours, followed by incubation in CY3 anti-rabbit secondary antisera raised in donkey (Jackson Immunoresearch, West Grove, PA; diluted 1:500) at room temperature for 90 minutes. 5-HT-neuron and Fos co-labeling was detected by incubating sections in primary antisera for tryptophan hydroxlase 2 (TPH2), the synthesizing enzyme for 5-HT) raised in sheep (Millipore, Billerica, MA, #AB1541) diluted 1:2000 and Fos raised in rabbit (EMD Chemicals, Gibbstown, NJ, #PC38) diluted 1:10,000 in PBS-BSA-TA at room temperature for 24 hours, followed by incubation in Alexa 488 anti-sheep (Invitrogen, Carlsbad, CA; diluted 1:500) and CY3 anti-rabbit (diluted 1:500) raised in donkey at room temperature for 90 minutes. Sections were rinsed, mounted, dried, and cover-slipped with a glycerol-based mounting medium.

SERT imaging and quantification of axon density

The density of SERT labeled axons was quantified from forebrain regions identified as having either altered 5-HT, 5-HT metabolite, or 5-HT turnover in HPLC experiments. Confocal image stacks (20 μm stack, 1 μm step-size, 1344 × 1024 pixel, 216 × 165 μm) were obtained using an Olympus spinning disk confocal microscope with a 40× oil objective, Hamamatsu Orca ER camera and Slidebook software (3i). Identical imaging parameters (neutral density filter, exposure time) were used on all samples. For each region, image stacks were randomly sampled per animal across at least two separate tissue sections (dorsal striatum, two images each from dorsal medial and dorsal lateral striatum; amygdala, three to four images from basolateral area). Quantification of axon density was performed using the protocol of Grider *et al.* (2006). This protocol semi-automatically detects linear structures in confocal images prior to thresholding, limiting the effect that the amount of labeled SERT protein within individual axon fibers might otherwise have on the quantification of total axon density in each image. Briefly, max projection images were created from confocal image stacks, opened in ImageJ/FIJI and converted to an 8-bit file. Background was subtracted using a rolling ball (50px) and curvilinear structures were detected using the Hessian filter of the Feature J plugin, selecting for the smallest eigen values (derivative = 1.0). The resulting eigen image was contrast enhanced (0.4% saturation), converted to binary, and thresholded (value = 175) to obtain a total pixel count of the area occupied by SERT-labeled axons. Individual measurements from each image were averaged for each subject to obtain a single mean value per region per animal, and mean values were compared between genotypes using independent samples t-test (significance at $p < .05$). As an

additional control to assess differences between genotypes in the amount of labeled SERT protein per individual axon fiber, three 30 μm axon segments were randomly sampled from each subject using the freehand selection tool in FIJI, and the total pixel area from each segments was quantified as described previously. Individual measurements were averaged for each subject and mean values were compared between genotypes using independent samples t-test (significance at $p < .05$).

5-HT neuron Fos analysis

For 5-HT neuron Fos analysis, tissue was systematically sampled by analyzing every third section through the entire rostral-caudal extent of the DRN (Paxinos and Franklin, 2001). Widefield images were obtained using an Olympus IX-81 fluorescence microscope with a 10× objective, a Hamamatsu Orca ER camera and Slidebook software (3i). Cells dually immunolabeled for Fos and TPH2 were counted within 6 discrete subregions of the DRN that are delineated across the rostral-caudal (3 regions defined relative to bregma: rostral, −4.16 to −4.24 mm; middle, −4.36 to −4.84 mm; caudal, −4.96 to −5.20 mm) and dorsal-ventral (2 regions defined by characteristic separation of immunolabeled 5-HT neurons) axes (Sperling and Commons, 2011). Dually labeled cells were manually enumerated by visualization of the individual and/or merged images of each channel in ImageJ. Analysis of every third section yielded two to three sections per region per animal, and counts for each section were averaged to yield a single per region mean value for each animal. Furthermore, the density of Tph2 immunofluroescent labeling was quantified in a subset of TS2-neo (n = 5) and WT (n = 5) mice to estimate the total number of Tph2 positive neurons between groups. Using ImageJ/FIJI the rostral-caudal and dorsal-ventral subregions were visually matched between subjects/groups and cropped to include the immediate rectangular area surrounding Tph2-positive cells (total image area, pixels). Images were thresholded (approximate value = 55) to select Tph2 fluorescence labeling with minimal background selection (total cell area in pixels), and the ratio of total cell area to total image area (Tph2 percentage) was quantified for each region per subject. For statistical analysis of 5-HT neuron Fos expression, a mixed-ANOVA with between subjects factors of genotype (TS2-neo or WT) and drug (saline or WAY) and within-subjects factor of DRN subregion was conducted on animal averages for each DRN subregion, and subsequent ANOVA within each DRN subregion. For comparisons between genotypes within each drug condition, independent-samples t-tests were conducted on each of six DRN subregions with significance determined after controlling the false-discovery rate at 5% (Benjamini-Hochberg correction, as previously described).

Results

To initially explore 5-HT system abnormalities in the TS2-neo mouse, we used HPLC to examine monoamine and metabolite tissue content in several forebrain structures implicated in the etiology of neurodevelopmental disorders: the orbitofrontal cortex, dorsal striatum, hippocampus, and amygdala (Figure 1A). Mixed-ANOVA revealed a significant main effect of genotype on 5-HT content ($F[1,17] = 4.494$, $p = .049$) and a trend for 5-HT turnover ($F[1,17] = 4.323$, $p = .053$), but not the metabolite 5-HIAA. Within specific forebrain regions, TS2-neo mice displayed a statistically significant increase in the tissue content of 5-

HT, but not 5-HIAA, in the dorsal striatum compared to WT mice ($t[17] = 3.014$, $p = .008$; $q = .047$) (Figure 1B, C). In contrast, TS2-neo mice also displayed a statistically significant decrease in 5-HT turnover in the amygdala compared to WT mice ($t[16] = 3.486$, $p = .003$) (Figure 1D). Alterations in 5-HT, 5-HIAA, and 5-HT turnover were similar in the orbital frontal cortex and dorsal hippocampus regions. Collectively, these results suggest regionally dependent 5-HT system abnormalities in TS2-neo mice, highlighted by an elevation in 5-HT content in the dorsal striatum and a disruption in 5-HT turnover in the amygdala of TS2-neo mice. Although the primary goal of the present research was to assess 5-HT system abnormalities, the tissue content of dopamine, norepinephrine, and their metabolites was also quantified. TS2-neo mice displayed an increase in dopamine ($t[15] = 2.708$, $p = .016$; $q = .048$) and a trend toward increased DOPAC ($t[15] = 2.977$, $p = .009$; $q = .054$) in the orbitofrontal cortex (Figure S1).

Elevation in 5-HT tissue content could reflect an increase in 5-HT synthesis or alternatively an increased density of dorsal striatum 5-HT axons innervating these forebrain regions. To assess this possibility, the density of immunofluorescently labeled SERT containing axons was quantified within both the dorsal striatum and amygdala of a subset of TS2-neo and WT mice: regions in which statistically significant alterations in 5-HT tissue content or 5-HT turnover ratio were observed, respectively. TS2-neo mice displayed an increased density of SERT-labeled axons within both the medial ($t[12] = 2.590$, $p = .024$) and lateral ($t[12] = 3.283$, $p = .007$) regions of the dorsal striatum (Figure 2A, 2B). In contrast, no differences in SERT-labeled axon density were observed in the amygdala of TS2-neo mice (Figure 2C, 2D). Finally, there was no difference between genotypes in SERT density within individual randomly sampled axons (TS2-neo, $M = 491.2$, $SD = 28.8$; WT, $M = 482.6$, $SD = 37.0$). Collectively, these results suggest that enhanced 5-HT axonal innervation of the dorsal striatum contributes to the elevated 5-HT tissue content observed in the dorsal striatum of TS2-neo mice, and reveals a regionally specific alteration of forebrain 5-HT axon innervation in TS2-neo mice.

Next, we examined whether TS2-neo mice display behavioral alterations that are reflective of disrupted ascending 5-HT system structure and/or functional activity. Stress-coping behavior (swimming) during the FST is a particularly illuminating behavioral endpoint to assess ascending 5-HT neuron activity and is disrupted in many mouse models of ASD (Commons *et al.*, 2017). Therefore, we utilized a 15-minute forced swim test to assess coping behavior in TS2-neo and WT mice. Mixed-ANOVA revealed a significant main effect of genotype on swimming behavior in saline treated mice ($F[1, 38] = 5.111$, $p = .030$), suggesting that TS2-neo mice swim significantly more during the 15-minute FST compared to their WT counterparts (Figure 3A), particularly during the first and second 5-minute epochs. To determine whether TS2-neo mice simply display a heightened level of general locomotor activity that would complicate interpretation of FST results, we also assessed open-field locomotor activity in a separate group of TS2-neo and WT mice, revealing no effects of genotype and/or time on open-field general locomotor activity nor on center-time (Figure 3B). Collectively, these results indicate an enhanced active coping response during an acute forced swim stress in TS2-neo mice.

Enhanced active coping behavior in the forced-swim may reflect disrupted regulation of ascending 5-HT system activity, including feedback-inhibition of the DRN 5-HT neurons (Commons 2008). Therefore, a separate group of TS2-neo and WT mice were administered the 5-HT1A antagonist WAY-100635 (WAY) just prior to the FST to quantify 5-HT1A dependent feedback inhibition of DRN 5-HT neurons in subsequent Fos experiments. This experimental design also allowed us to assess stress coping behavior in these mice. Following acute administration of WAY, mixed-ANOVA revealed a significant interaction between time and drug on swimming behavior ($F[2, 110] = 6.445$, $p = .002$) but no statistically significant interaction with genotype, suggesting that acute administration of the 5-HT1A antagonist WAY enhances swimming behavior in both TS2-neo and WT mice across a 15-minute FST (Figure 3A).

It is well established that acute stress alters the activity pattern of ascending 5-HT neurons arising from the DRN, in which Fos expression is elevated within anatomically defined rostral-caudal and dorsal-ventral DRN subregions (Figure 4A), while overall 5-HT neuron activity is dampened via somatodendritically located inhibitory 5-HT1A receptors (5-HT1A dependent feedback inhibition) (Commons, 2008). Therefore, we characterized 5-HT neuron Fos activity within anatomically defined DRN subregions in both FST and FST+WAY exposed TS2-neo and WT mice (Figure 4B). Under the latter condition, the novel expression of Fos following WAY treatment is indicative of prior inhibition of 5-HT neurons through a 5-HT1A dependent feedback mechanism (Commons, 2008). Mixed-ANOVA revealed a significant genotype by subregion interaction ($F[5,196] = 5.262$, $p < .001$), a significant drug by subregion interaction ($F[5,196] = 28.724$, $p < .001$), and a trend towards a genotype by drug by subregion interaction ($F[5, 196] = 1.855$, $p = .010$). Follow-up ANOVAs within DRN subregions revealed a significant main effect of genotype in the caudal-ventral ($F[1,37] = 10.774$, $p = .002$) and rostral-dorsal ($F[1,37] = 19.070$, $p = .0001$) subregions of the DRN and a genotype by drug interaction exclusively in the rostral-dorsal DRN ($F[1,37] = 5.949$, $p = .02$). Specifically, saline-treated TS2-neo mice display a significantly increased number of Fos-positive 5-HT neurons in the caudal-ventral DRN compared to their WT counterparts ($t[24] = 3.164$, $p = .004$, $q = .024$), and a trend toward increased Fos-positive 5-HT neurons in the rostral-dorsal DRN ($t[22] = 2.36$, $p = .028$, $q = .084$) (Figure 4C, 4E). When WAY is administered prior to the FST, Fos expression is enhanced in all DRN subregions of both TS2-neo and WT mice, indicative of intact 5-HT1A dependent feedback inhibition. However, this WAY-induced elevation in Fos positive 5-HT neurons is significantly greater in the rostral-dorsal DRN of TS2-neo mice compared to WT mice (genotype within WAY, $t[16] = 3.330$, $p = .004$, $q = .024$). Furthermore, WAY treated TS2-neo mice maintain an increased number of Fos-positive 5-HT neurons in the caudal-ventral DRN compared to WAY treated WT mice ($t [16] = 2.152$, $p = .047$, $q = .141$) (Figure 4D, 4E). Importantly, the total amount of Tph2 immunofluorescent labeling was identical between TS2-neo and WT mice across all DRN subregions examined (Figure S2), suggesting that the increased number of Fos-positive Tph2 neurons, as well as increased 5HT axon density, is unlikely to be the result of an increased number of 5HT neurons. Collectively, these results reveal enhanced 5-HT neural activity in the caudal-ventral DRN and enhanced 5-HT1A-dependent feedback inhibition of the rostral-dorsal DRN in TS2-neo mice following an acute forced swim stress.

Discussion

The ascending 5-HT system is a neural circuit implicated in a broad range of human neuropsychiatric and neurodevelopmental disorders, including depression, bipolar, schizophrenia, and autism spectrum disorders, yet how serotonin is impaired in each of these disorders remains poorly understood. Similarly, polymorphism in the gene *CACNA1C,* which codes for the Cav1.2 L-type calcium channel, represents a significant risk locus across this same spectrum. In the present study we have revealed pleotropic effects on the 5-HT system in the TS2-neo mouse model of ASD that contains a global gain of function mutation in the Cav1.2 channel, including enhanced forebrain 5-HT axonal innervation of the dorsal striatum, disrupted 5-HT metabolism in the amygdala, an enhanced active coping response to acute stress, and overactivity/disrupted feedback inhibition of dorsal raphe 5-HT neurons. These results provide further evidence for 5-HT's involvement in ASD and extend this evidence by implicating regionally dependent alterations in the mid/hindbrain dorsal raphe system and in its forebrain projection targets. Finally, these results identify a neural circuit in the 5-HT system in which to explore the role of *CACNA1C* and Cav1.2 LTCCs in the etiology or treatment of neuropsychiatric and developmental disorders.

Cav1.2 channels are important regulators of calcium signaling and gene expression in the developed brain (Ma *et al.*, 2012) that are also critical to brain development, being differentially expressed (both spatially and temporally) in the central nervous system across vertebrate embryonic development (Lewis *et al.*, 2009; Moreau *et al.*, 2016). The TS2-neo mouse is heterozygous for a global gain function mutation in Cav1.2 that would also be present throughout embryonic development, and disrupted calcium signaling in this mouse model has the potential to alter brain development beginning at early embryonic stages. Previous research has shown a range of neural structure abnormalities appearing in the developed mouse brain following Cav1.2 knockout, including an altered pattern of hippocampal neurogenesis (Völkening *et al.*, 2017) and oligodendrocyte development that disrupts postnatal myelination (Cheli *et al.*, 2016). More specifically in the TS2-neo mouse, dendritic retraction is observed in forebrain primary neurons (Krey *et al.*, 2013) as well as an overall asymmetrical brain appearance compared to wild-type littermates, suggesting subtle alterations in brain development in these mice (Bett *et al.*, 2012). The present results extend these findings by revealing regionally dependent alterations in 5-HT axonal innervation of the dorsal striatum and provide the first report of altered monoaminergic structure (and function) associated with the TS2 mutation. Whether increased 5-HT innervation of the dorsal striatum contributes to the overall behavioral profile of TS2-neo mice is currently unknown. However, acute stress has been shown to promote dorsal striatum dependent "habit" memory while disrupting hippocampus dependent "cognitive" memory (Schwabe & Wolfe, 2012; Schwabe, 2013), which may contribute to the perseverative behavior that is characteristic of TS2-neo mice in the water Y-maze task (Bader *et al.*, 2011). The role of ascending 5-HT system structure and stress induced 5-HT activity on dorsal striataum-dependent behavior remains an important area for further study.

ASD is often associated with a disrupted behavioral response to acute stress and/or difficulty adapting to change (García-Villamisar & Rojahn, 2015). For example, individuals with ASD often display rumination and an enhanced state of emotional arousal that is reflective of

disrupted emotion regulation (Mazefsky *et al.*, 2014). Furthermore, lowered ability in adapting to and coping with stressors is strongly associated with an increased severity of classic ASD behaviors including self injury, stereotypy and irritability (Williams *et al.*, 2017). The FST behavioral paradigm provides unique insight into stress coping strategy and can be utilized to assess this neurobehavioral feature in genetic mouse models related to ASD. Specifically, mice typically exhibit a natural shift from predominantly active to more passive coping strategies over time in the FST. In the present study, we reveal an enhanced and sustained active coping response in TS2-neo mice during a prolonged acute forced swim stress. This finding is unlikely to be attributable to differences in weight or general locomotor activity (which were similar between TS2-neo and WT mice in the present study), nor to general disruptions in gross motor behavior which appear normal in TS2-neo mice according to previous studies (Bader *et al.*,2011). This data supports previous findings of enhanced active coping strategies to acute stressors across several other mouse models related to ASD, including Fragile X mental retardation 1 knockout, BTBR, and 16p11.2 microdeletion mouse models (Guo & Commons, 2017; Onaivi *et al.*, 2011; Silverman *et al.*, 2010; Uutela *et al.*, 2014). Interestingly, enhanced passive, rather than active, coping strategies are observed in several other mouse models related to ASD including Engrailed 2 null mice, GAP43 knockout, and Grik4 overexpressing mice (Brielmaier *et al.*, 2012; Zaccaria *et al.*, 2010; Aller *et al.*, 2015). There is little evidence in either the animal or human ASD literature to support the interpretation of either enhanced active or passive coping response in the FST with respect to depression or mood (for review, see Commons *et al.*, 2017), and therefore the present results are most accurately interpreted as a disruption to the acute stress response and/or typical pattern of stress adaptation in TS2-neo mice. Our results provide further evidence for the utility of the FST in providing insight into the neurobehavioral features of ASD, and further point towards disrupted adaptive coping response as an underexplored endophenotype in ASD genetic mouse models.

Acute stress influences the activity of DRN 5-HT neurons, particularly in the caudal portion of the DRN (Commons, 2008). Here, we reveal that TS2-neo mice display an increased number of Fos positive 5-HT neurons within the caudal-ventral subregion compared to their WT littermates, indicative of a regionally-dependent alteration in DRN 5-HT neurons following an acute forced-swim stress. Previous work has suggested that overactivity of the caudal DRN is associated with negatively reinforcing stimuli, and therefore this neural feature provides a correlate of the enhanced active coping response observed in TS2-neo mice (Sperling & Commons, 2011). We have recently observed this same pattern of enhanced caudal DRN 5-HT neuron activity in the BTBR mouse that also exhibits excessive active coping in the FST (Guo & Commons, Autism Research 2017). Additionally, the ASD related gene *Met* is preferentially expressed within the caudal DR and its selective deletion from these serotonin neurons produces a deficit in social interaction (Okaty *et al.*, 2015). This latter finding is particularly intriguing, as a social interaction deficit may potentially reflect an aversion to or exaggerated stress response when faced with novel social contact (Beery & Kaufer, 2015). While differential expression of *Cacna1c* or Cav1.2 channels has not been observed across the rostral-caudal axis of the DRN, the present results suggest that the global gain of function mutation in TS2-neo mice produces an overactivity of the caudal DRN that may represent a common neural signature across ASD mouse models.

Furthermore, the caudal DRN emerges as a particularly interesting neuroanatomical locus in which to explore the interaction of stress with classic behavioral phenotypes that define genetic mouse models related to ASD, including deficits in social interaction, perseverative behavior, and vocalization abnormalities.

Additionally, the present study reveals that the increased caudal DRN 5-HT neuron activity is accompanied by enhanced 5-HT1A dependent feedback-inhibition of the rostral DRN. Specifically, the increased number of Fos-positive rostral DRN 5-HT neurons following blockade of 5-HT1A receptors in TS2-neo mice reflects enhanced prior inhibition through a 5-HT1A-dependent mechanism (Commons, 2008). Importantly, the caudal and rostral DRN are functionally and structurally distinct, as they are differentially activated by negative and positive reinforcing stimuli (respectively) and each possess unique efferent forebrain targets. That is, projections of the caudal DRN most prominently influence classic forebrain stress-circuitry, including the septum and hippocampus, while rostral DRN projections most prominently influencing forebrain regions associated with emotion and motivation, including the amygdala and nucleus accumbens (Commons, 2016). In fact, the enhanced feedback-inhibition observed in the rostral DRN of TS2-neo mice is consistent with the reduction in amygdala 5-HT turnover that is also revealed in the present study. Additional experiments are needed to directly assess the contribution of rostral DRN functional activity to changes in amygdala 5-HT metabolism. However, the present results are consistent with disrupted feedback-inhibitory control over the rostral and caudal components of the ascending 5-HT system in the TS2-neo mouse. Given emerging evidence for the role of the ascending 5-HT system in the expression/maintenance of cognitive flexibility in the face of environmental challenge (Matias *et al.*, 2017), these regionally specific abnormalities in 5-HT system structure and function are likely to contribute to the neurobehavioral features of ASD.

TS2-neo mice contain a global gain of function mutation in *Cacna1c*, and therefore both direct and indirect mechanisms are likely to contribute to the behavioral features and 5-HT system alterations reported in the present study. Cav1.2 expression is highest in cortical and hippocampal regions, and the TS2-neo mutation is specifically associated with increased neural activity in primary neurons (Krey *et al.*, 2013; Li *et al.*, 2016). However, L-type calcium channels are also expressed directly on 5-HT neurons where they play a unique role in activity-dependent and local dendritic 5-HT release within the DRN to provide 5-HT1A dependent inhibitory feedback of DRN 5-HT neuron activity (Colgan *et al.*, 2012). Therefore, the present results are consistent with an increase in forebrain excitatory drive of the DRN coupled with enhanced local feedback-inhibition of 5-HT neurons, a hypothesis that can be explored in future experiments.

Finally, the present results reveal a 5-HT neuron phenotype that is associated with the TS2-neo mutation and that may apply across other mouse models related to ASD. However, a broader implication that arises from the present study is that Cav1.2 L-type calcium channels influence the neural circuitry of the acute stress response. In humans, polymorphisms of *CACNA1C* are associated with increased risk for development of a broad range of neuropsychiatric disorders, including depression, schizophrenia, and bipolar disorder, and stress plays a crucial role in both the development and exacerbation of behaviorial symptoms

in each of these conditions (Cross-Disorder Group of the Psychiatric Genomics Consortium, 2013; Hankin & Abela, 2005.). Given the role of L-type calcium channels in local regulation of 5-HT neuron activity, it is possible that polymorphisms in *CACNA1C* also influence the function of 5-HT neurons in response to stress. Therefore, the ascending 5-HT system emerges as an intriguing location for the neural circuitry of a gene (e.g. *CACNA1C*) by environment (e.g. stress) interaction in the etiology of neuropsychiatric disorder.

The identification of neural circuits that are disrupted across genetic mouse models of ASD, and across different neurological disorders, is critical for the translation of findings in animal models that can be applied to the extremely heterogeneous conditions in humans. We provide evidence for regionally dependent alterations in ascending 5-HT system structure and function in the TS2-neo genetic mouse model of ASD. These data add to a growing body of research suggesting 5-HT system involvement in both animal models and in the human condition.

Supplementary Material

Refer to Web version on PubMed Central for supplementary material.

Acknowledgments

Funding was provided by the National Institutes of Health grants DA021801 and HD036379 (KGC), the Brain and Behavior Foundation NARSAD Independent Investigator Award (KGC), the Sara Page Mayo Foundation for Pediatric Pain Research (KGC), and the Anesthesia Research Distinguished Trailblazer Award (DGE). We thank Christopher Panzini for assistance conducting the research.

Abbreviations

5-HIAA	5-Hydroxyindoleacetic acid
5-HT	5-hydroxytryptamine
5-HT1A	5-HT type 1A receptors
ASD	autism spectrum disorder
DRN	dorsal raphe nuclei
FDR	False-discovery rate
FST	forced-swim test
SERT	serotonin transporter
Tph2	tryptophan hydroxylase 2
WAY	WAY-100635

References

Aller MI, Pecoraro V, Paternain AV, Canals S, Lerma J. Increased Dosage of High-Affinity Kainate Receptor Gene grik4 Alters Synaptic Transmission and Reproduces Autism Spectrum Disorders Features. J Neurosci. 2015; 35:13619–13628. [PubMed: 26446216]

Bachevalier J, Loveland KA. The orbitofrontal–amygdala circuit and self-regulation of social–emotional behavior in autism. Neurosci Biobehav Rev. 2006; 30:97–117. [PubMed: 16157377]

Bader PL, Faizi M, Kim LH, Owen SF, Tadross MR, Alfa RW, Bett GCL, Tsien RW, Rasmusson RL, Shamloo M. Mouse model of Timothy syndrome recapitulates triad of autistic traits. Proc Natl Acad Sci USA. 2011; 108:15432–15437. [PubMed: 21878566]

Beery AK, Kaufer D. Stress, social behavior, and resilience: Insights from rodents. Neurobiol Stress. 2014; 1:116–127.

Benjamini Y, Hochberg Y. Controlling the false discovery rate: a practical and powerful approach to multiple testing. J R Statist Soc B. 1995; 57:289–300.

Bett GC, Lis A, Wersinger SR, Baizer JS, Duffey ME, Rasmusson RL. A Mouse Model of Timothy Syndrome: a Complex Autistic Disorder Resulting from a Point Mutation in Cav1.2. N Am J Med Sci (Boston). 2012; 5:135–140. [PubMed: 24371506]

Brielmaier J, Matteson PG, Silverman JL, Senerth JM, Kelly S, Genestine M, Millonig JH, DiCicco-Bloom E, Crawley JN. Autism-relevant social abnormalities and cognitive deficits in engrailed-2 knockout mice. PLoS ONE. 2012; 7:e40914. [PubMed: 22829897]

Cheli VT, Santiago González DA, Namgyal Lama T, Spreuer V, Handley V, Murphy GG, Paez PM. Conditional Deletion of the L-Type Calcium Channel Cav1.2 in Oligodendrocyte Progenitor Cells Affects Postnatal Myelination in Mice. J Neurosci. 2016; 36:10853–10869. [PubMed: 27798140]

Colgan LA, Cavolo SL, Commons KG, Levitan ES. Action potential-independent and pharmacologically unique vesicular serotonin release from dendrites. J Neurosci. 2012; 32:15737–15746. [PubMed: 23136413]

Commons KG. Evidence for topographically organized endogenous 5-HT-1A receptor-dependent feedback inhibition of the ascending serotonin system. Eur J Neurosci. 2008; 27:2611–2618. [PubMed: 18513318]

Commons KG. Ascending serotonin neuron diversity under two umbrellas. Brain Struct Funct. 2016; 221:3347–3360. [PubMed: 26740230]

Commons KG, Cholanians AB, Babb JA, Ehlinger DG. The Rodent Forced Swim Test Measures Stress-Coping Strategy, Not Depression-like Behavior. ACS Chem Neurosci. 2017; 8:955–960. [PubMed: 28287253]

Cross-Disorder Group of the Psychiatric Genomics Consortium. Identification of risk loci with shared effects on five major psychiatric disorders: a genome-wide analysis. Lancet. 2013; 381:1371–1379. [PubMed: 23453885]

Cryan JF, Valentino RJ, Lucki I. Assessing substrates underlying the behavioral effects of antidepressants using the modified rat forced swimming test. Neurosci Biobehav Rev. 2005; 29:547–569. [PubMed: 15893822]

Fletcher A, Forster EA, Bill DJ, Brown G, Cliffe IA, Hartley JE, Jones DE, McLenachan A, Stanhope KJ, Critchley DJ, Childs KJ, Middlefell VC, Lanfumey L, Corradetti R, Laporte AM, Gozlan H, Hamon M, Dourish CT. Electrophysiological, biochemical, neurohormonal and behavioural studies with WAY-100635, a potent, selective and silent 5-HT1A receptor antagonist. Behav Brain Res. 1996; 73:337–353. [PubMed: 8788530]

Fuccillo MV. Striatal Circuits as a Common Node for Autism Pathophysiology. Front Neurosci. 2016; 10:27. [PubMed: 26903795]

García-Villamisar D, Rojahn J. Comorbid psychopathology and stress mediate the relationship between autistic traits and repetitive behaviours in adults with autism. J Intellect Disabil Res. 2015; 59:116–124. [PubMed: 23919538]

Gould GG, Hensler JG, Burke TF, Benno RH, Onaivi ES, Daws LC. Density and function of central serotonin (5-HT) transporters, 5-HT1A and 5-HT2A receptors, and effects of their targeting on BTBR T+tf/J mouse social behavior. J Neurochem. 2011; 116:291–303. [PubMed: 21070242]

Green EK, Grozeva D, Jones I, Jones L, Kirov G, Caesar S, Gordon-Smith K, Fraser C, Forty L, Russell E, Hamshere ML, Moskvina V, Nikolov I, Farmer A, McGuffin P, Holmans PA, Owen MJ, O'Donovan MC, Craddock N. Wellcome Trust Case Control Consortium. The bipolar disorder risk allele at CACNA1C also confers risk of recurrent major depression and of schizophrenia. Mol Psychiatry. 2010; 15:1016–1022. [PubMed: 19621016]

Grider MH, Chen Q, Shine HD. Semi-automated quantification of axonal densities in labeled CNS tissue. J Neurosci Methods. 2006; 155:172–179. [PubMed: 16469388]

Guo YP, Commons KG. Serotonin neuron abnormalities in the BTBR mouse model of autism. Autism Res. 2017; 10:66–77. [PubMed: 27478061]

Hankin, BL., Abela, JRZ. Development of Psychopathology: A Vulnerability-Stress Perspective. SAGE Publications; 2005.

Kane MJ, Angoa-Peréz M, Briggs DI, Sykes CE, Francescutti DM, Rosenberg DR, Kuhn DM. Mice genetically depleted of brain serotonin display social impairments, communication deficits and repetitive behaviors: possible relevance to autism. PLoS ONE. 2012; 7:e48975. [PubMed: 23139830]

Kerr TM, Muller CL, Miah M, Jetter CS, Pfeiffer R, Shah C, Baganz N, Anderson GM, Crawley JN, Sutcliffe JS, Blakely RD, Veenstra-Vanderweele J. Genetic background modulates phenotypes of serotonin transporter Ala56 knock-in mice. Mol Autism. 2013; 4:35. [PubMed: 24083388]

Krey JF, Paşca SP, Shcheglovitov A, Yazawa M, Schwemberger R, Rasmusson R, Dolmetsch RE. Timothy syndrome is associated with activity-dependent dendritic retraction in rodent and human neurons. Nat Neurosci. 2013; 16:201–209. [PubMed: 23313911]

Laviola G, Macrì S, Morley-Fletcher S, Adriani W. Risk-taking behavior in adolescent mice: psychobiological determinants and early epigenetic influence. Neurosci Biobehav Rev. 2003; 27:19–31. [PubMed: 12732220]

Levy SE, Mandell DS, Schultz RT. Autism. Lancet. 2009; 374:1627–1638. [PubMed: 19819542]

Lewis BB, Wester MR, Miller LE, Nagarkar MD, Johnson MB, Saha MS. Cloning and characterization of voltage-gated calcium channel alpha1 subunits in Xenopus laevis during development. Dev Dyn. 2009; 238:2891–2902. [PubMed: 19795515]

Li B, Tadross MR, Tsien RW. Sequential ionic and conformational signaling by calcium channels drives neuronal gene expression. Science. 2016; 351:863–867. [PubMed: 26912895]

Lidov HG, Molliver ME. Immunohistochemical study of the development of serotonergic neurons in the rat CNS. Brain Res Bull. 1982; 9:559–604. [PubMed: 6756556]

Liu Q, Wong-Riley MTT. Postnatal changes in tryptophan hydroxylase and serotonin transporter immunoreactivity in multiple brainstem nuclei of the rat: implications for a sensitive period. J Comp Neurol. 2010; 518:1082–1097. [PubMed: 20127812]

Ma H, Cohen S, Li B, Tsien RW. Exploring the dominant role of Cav1 channels in signalling to the nucleus. Biosci Rep. 2012; 33:97–101. [PubMed: 23088728]

Matias S, Lottem E, Dugué GP, Mainen ZF. Activity patterns of serotonin neurons underlying cognitive flexibility. Elife. 2017:6.

Mazefsky CA, Borue X, Day TN, Minshew NJ. Emotion regulation patterns in adolescents with high-functioning autism spectrum disorder: comparison to typically developing adolescents and association with psychiatric symptoms. Autism Res. 2014; 7:344–354. [PubMed: 24610869]

Moreau M, Néant I, Webb SE, Miller AL, Riou JF, Leclerc C. Ca(2+) coding and decoding strategies for the specification of neural and renal precursor cells during development. Cell Calcium. 2016; 59:75–83. [PubMed: 26744233]

Mosienko V, Beis D, Pasqualetti M, Waider J, Matthes S, Qadri F, Bader M, Alenina N. Life without brain serotonin: reevaluation of serotonin function with mice deficient in brain serotonin synthesis. Behav Brain Res. 2015; 277:78–88. [PubMed: 24928769]

Muller CL, Anacker AMJ, Veenstra-VanderWeele J. The serotonin system in autism spectrum disorder: From biomarker to animal models. Neuroscience. 2016; 321:24–41. [PubMed: 26577932]

Okaty BW, Freret ME, Rood BD, Brust RD, Hennessy ML, deBairos D, Kim JC, Cook MN, Dymecki SM. Multi-Scale Molecular Deconstruction of the Serotonin Neuron System. Neuron. 2015; 88:774–791. [PubMed: 26549332]

Onaivi ES, Benno R, Halpern T, Mehanovic M, Schanz N, Sanders C, Yan X, Ishiguro H, Liu QR, Berzal AL, Viveros MP, Ali SF. Consequences of cannabinoid and monoaminergic system disruption in a mouse model of autism spectrum disorders. Curr Neuropharmacol. 2011; 9:209–214. [PubMed: 21886592]

Paxinos, G., Franklin, K. The Mouse Brain in Stereotaxic Coordinates. 4. Academic Press; New York, NY: 2012.

Schain RJ, Freedman DX. Studies on 5-hydroxyindole metabolism in autistic and other mentally retarded children. J Pediatr. 1961; 58:315–320. [PubMed: 13747230]

Schwabe L. Stress and the engagement of multiple memory systems: integration of animal and human studies. Hippocampus. 2013; 23:1035–1043. [PubMed: 23929780]

Schwabe L, Wolf OT. Stress modulates the engagement of multiple memory systems in classification learning. J Neurosci. 2012; 32:11042–11049. [PubMed: 22875937]

Silverman JL, Yang M, Turner SM, Katz AM, Bell DB, Koenig JI, Crawley JN. Low stress reactivity and neuroendocrine factors in the BTBR T+tf/J mouse model of autism. Neuroscience. 2010; 171:1197–1208. [PubMed: 20888890]

Sperling R, Commons KG. Shifting topographic activation and 5-HT1A receptor-mediated inhibition of dorsal raphe serotonin neurons produced by nicotine exposure and withdrawal. Eur J Neurosci. 2011; 33:1866–1875. [PubMed: 21501256]

Splawski I, Timothy KW, Decher N, Kumar P, Sachse FB, Beggs AH, Sanguinetti MC, Keating MT. Severe arrhythmia disorder caused by cardiac L-type calcium channel mutations. Proc Natl Acad Sci USA. 2005; 102:8089–8096. discussion 8086–8088. [PubMed: 15863612]

Splawski I, Timothy KW, Sharpe LM, Decher N, Kumar P, Bloise R, Napolitano C, Schwartz PJ, Joseph RM, Condouris K, Tager-Flusberg H, Priori SG, Sanguinetti MC, Keating MT. Ca(V)1.2 calcium channel dysfunction causes a multisystem disorder including arrhythmia and autism. Cell. 2004; 119:19–31. [PubMed: 15454078]

Uutela M, Lindholm J, Rantamäki T, Umemori J, Hunter K, Võikar V, Castrén ML. Distinctive behavioral and cellular responses to fluoxetine in the mouse model for Fragile X syndrome. Front Cell Neurosci. 2014; 8:150. [PubMed: 24904293]

Veenstra-VanderWeele J, Muller CL, Iwamoto H, Sauer JE, Owens WA, Shah CR, Cohen J, Mannangatti P, Jessen T, Thompson BJ, Ye R, Kerr TM, Carneiro AM, Crawley JN, Sanders-Bush E, McMahon DG, Ramamoorthy S, Daws LC, Sutcliffe JS, Blakely RD. Autism gene variant causes hyperserotonemia, serotonin receptor hypersensitivity, social impairment and repetitive behavior. Proc Natl Acad Sci USA. 2012; 109:5469–5474. [PubMed: 22431635]

Völkening B, Schönig K, Kronenberg G, Bartsch D, Weber T. Deletion of psychiatric risk gene Cacna1c impairs hippocampal neurogenesis in cell-autonomous fashion. Glia. 2017; 65:817–827. [PubMed: 28230278]

Williams DL, Siegel M, Mazefsky CA. Autism and Developmental Disorders Inpatient Research Collaborative (ADDIRC). Problem Behaviors in Autism Spectrum Disorder: Association with Verbal Ability and Adapting/Coping Skills. J Autism Dev Disord. 2017 In press.

Zaccaria KJ, Lagace DC, Eisch AJ, McCasland JS. Resistance to change and vulnerability to stress: autistic-like features of GAP43-deficient mice. Genes Brain Behav. 2010; 9:985–996. [PubMed: 20707874]

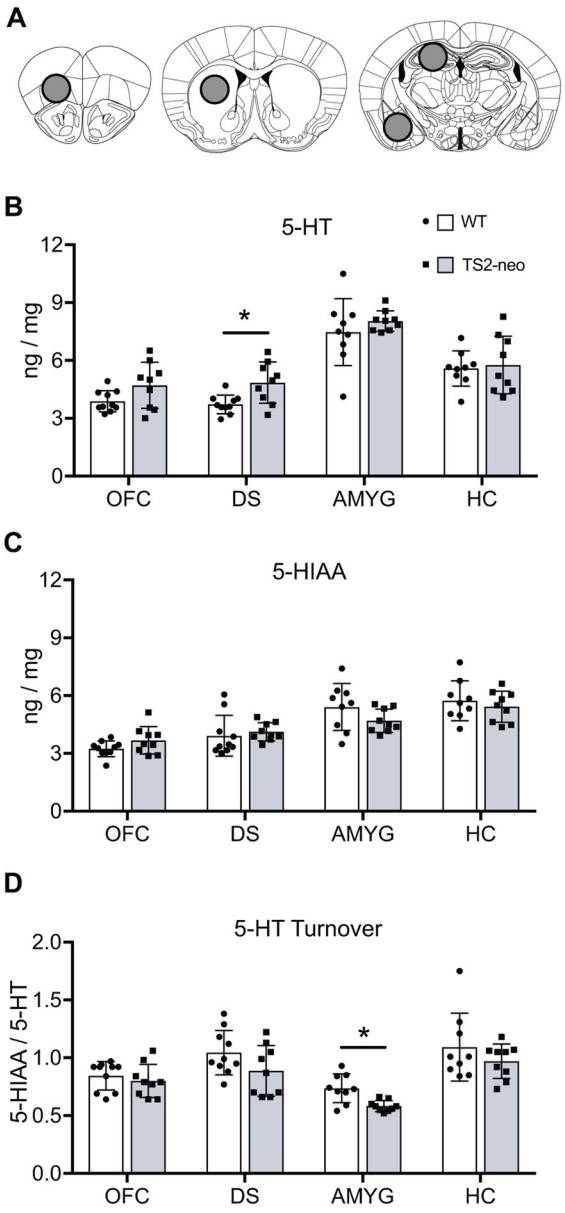

Figure 1.

HPLC analysis of 5-HT, metabolite 5-HIAA, and 5-HT turnover. ***A***, Location of tissue collection for analysis, including the orbitofrontal cortex (OFC, left), dorsal striatum (DS, middle), hippocampus (HC) and amygdala (AMYG) regions (right). ***B–D,*** quantified as nanograms of biogenic amine per milligram of tissue, ±SD. *, FDR-adjusted $q < .05$.

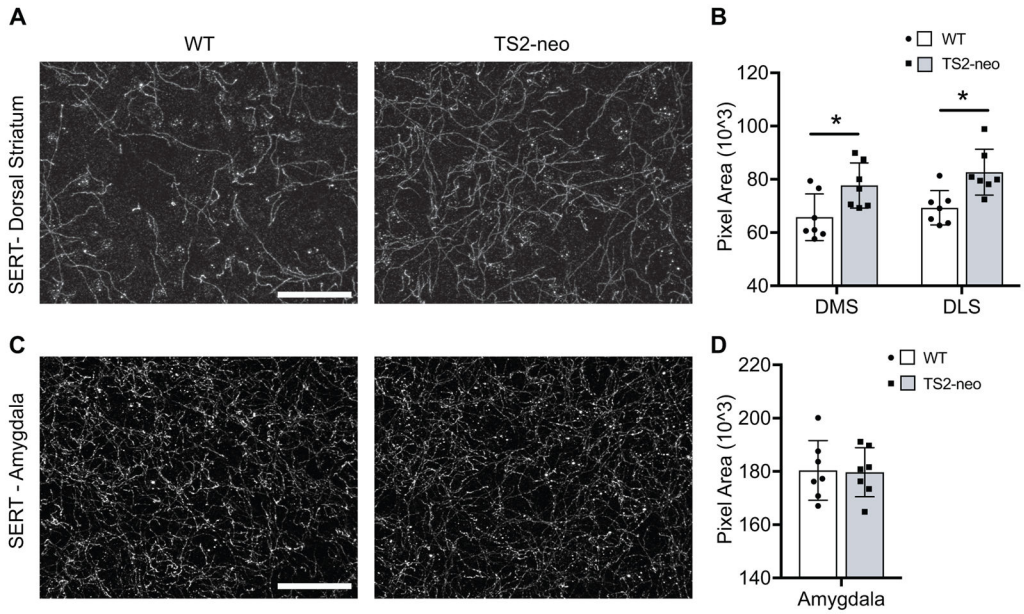

Figure 2.

Density of forebrain 5-HT axon innervation. ***A***, SERT immunolabeling of dorsal striatum from WT and TS2-neo mice. Scale bar, 50μm. ***B***, quantification of axon density from the dorsal medial (DMS) and dorsal lateral (DLS) subregions, ±SD. *****, $p < .05$. ***C***, SERT immunolabeling of dorsal striatum from WT and TS2-neo mice. Scale bar, 50μm. ***D***, quantification of axon density from the basolateral amygdala.

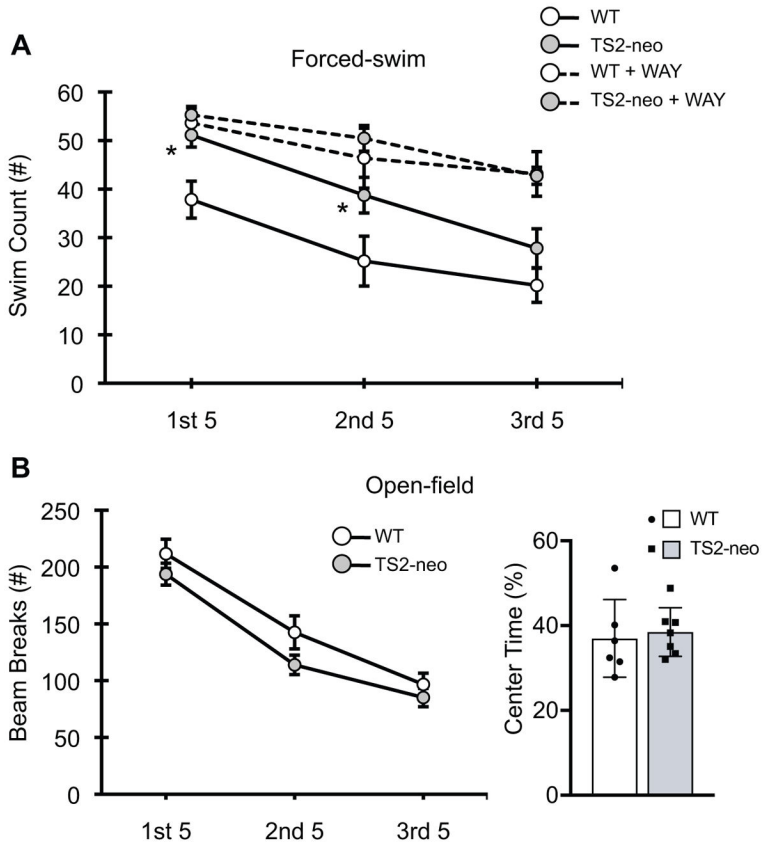

Figure 3.

Behavioral measures in WT and TS2-neo mice. ***A*** Forced swim test swim count (active coping behavior) measured across 5-minute time bins, ±SEM. ***B*** Overall open-field locomotor activity measured measured across 5-minute time bins, ±SEM (left) and total time spent in the center rectangle of the testing chamber, ±SD (right). *****, $p < .05$.

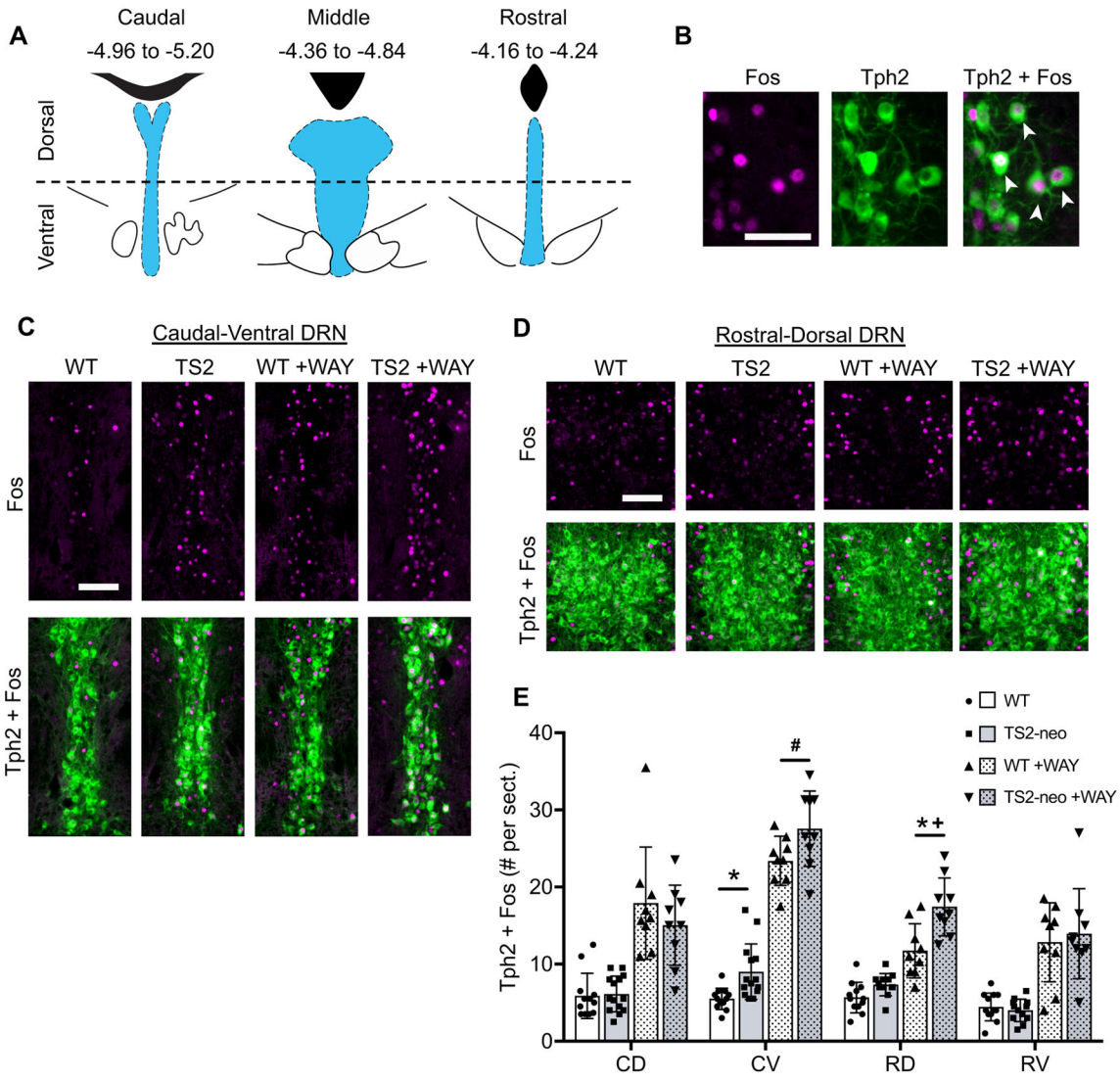

Figure 4.

Dorsal raphe nuclei (DRN) 5-HT neuron activity and 5-HT1A dependent feedback inhibition following forced swim in WT and TS2-neo mice. ***A***, Location of the DRN (blue) relative to the 4th ventricle or cerebral aqueduct (black), and bregma coordinates of DRN subregions delineated across the rostral-caudal and dorsal-ventral axes. ***B***, Representative DRN neurons immunofluorescently labeled for Fos (magenta, left) and Tph2 (green, middle). White arrows in the merged image (right) indicate double-labeled cells. Scale bar, 50μm. ***C–D***, Immunofluorescent labeling of Fos (top) and merged images of Fos + Tph2 (bottom), with and without administration of 5-HT1A antagonist WAY-100635 (WAY), Scale bars, 100μm. ***E***, Average # of Fos+Tph2 cells counted per tissue section from DRN subregions, ±SD. CD = caudal-dorsal, CV = caudal-ventral, RD = rostral-dorsal, RV = rostral-ventral. *, FDR-adjusted $q < .05$ between TS2-neo and corresponding WT control group. #, $p < .05$ and $q > .05$ between TS2-neo and corresponding WT control. +, genotype by drug interaction $p < .05$.